

# Investigating the Subfunctionalization of Two *Xenopus Laevis* AHR1 Paralogs

Eric Engelbrecht '14 with mentor Wade Powell

Kenyon College Summer Science 2013

## Abstract

The aryl hydrocarbon receptor (AHR) is well known for mediating the toxic effects of environmental contaminants like 2,3,7,8-tetrachlorodibenzo-*p*-dioxin (TCDD). We are interested in defining the molecular mechanisms underlying AHR signaling in *Xenopus laevis*, a frog widely used in studies of vertebrate development and developmental. *X. laevis* experienced a relatively recent genomic duplication (~40 million years ago) resulting in the emergence of many paralogous genes, including AHR paralogs AHR1 $\alpha$  and AHR1 $\beta$ . Several lines of evidence suggest unique functions for each AHR, including significant sequence divergence and distinct tissue-specific expression patterns. We aimed to test the hypothesis that AHR1 $\alpha$  and AHR1 $\beta$  have subfunctionalized roles of the ancestral AHR gene. siRNA knockdown of AHR1 $\beta$  suggests that it is partially responsible for induction of CYP1A6, the primary AHR-mediated gene, by TCDD. Using custom TALENs, we have engineered the genome of XLK-WG cells to knockout AHR1 $\alpha$  expression. This mutant cell line awaits functional characterization.

## AHR Pathway

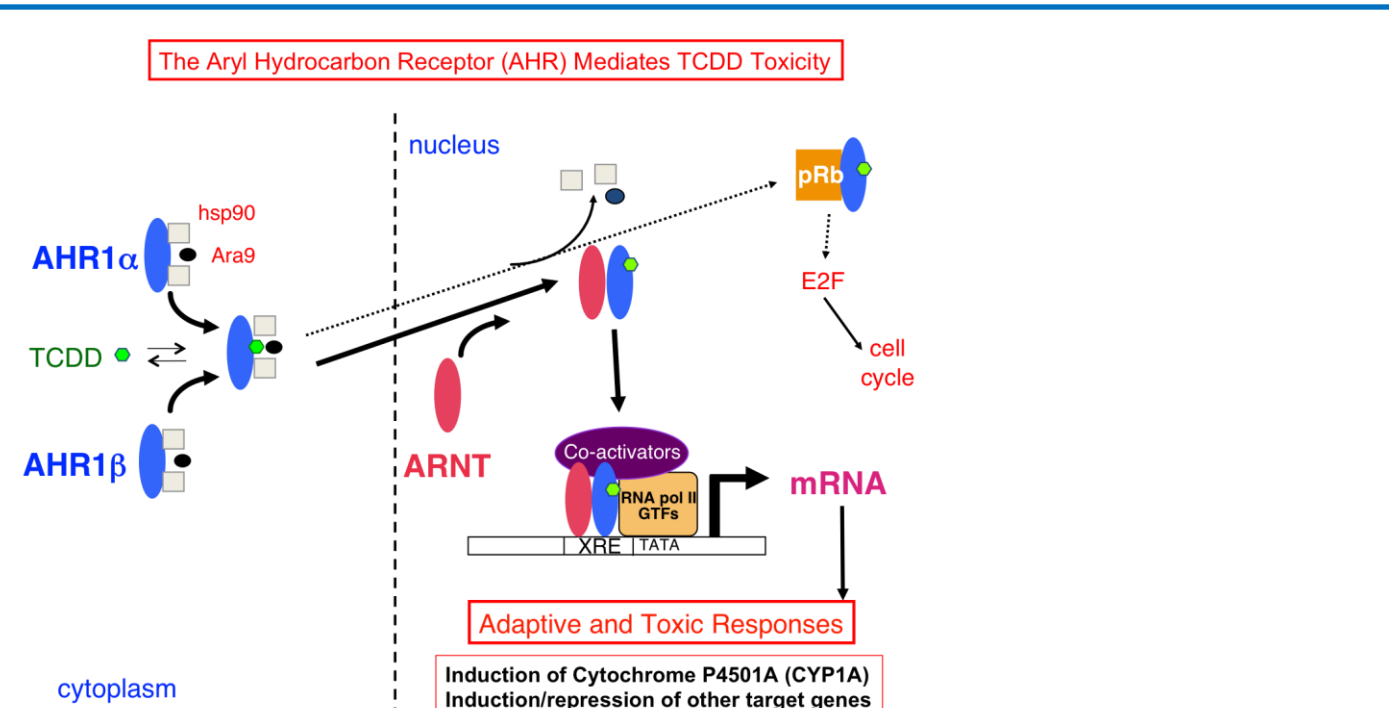


**Figure 1. The AHR pathway.** AHR1 $\alpha$  and AHR1 $\beta$  exist in an inactive state in the cytoplasm. Upon ligand binding, each receptor moves to the nucleus and forms a transcriptionally active heterodimer with Ah receptor nuclear translocator (ARNT) to induce expression of target genes. Alterations in gene expression likely underlies toxicity of AHR agonists.

## Methods Overview

### 1. siRNA Knockdown

Using siRNAs, we knocked down mRNA expression of each paralog in XLK-WG cells, a cell line derived from *X. laevis* kidney epithelium. While the siRNA targeting AHR1 $\beta$  achieved 90% knockdown of its target gene and did not affect AHR1 $\alpha$  expression, the siRNA targeting AHR1 $\alpha$  achieved 65% knockdown of its target and 52% knockdown of AHR1 $\beta$ , an undesired off-target effect. We measured the expression of a classic AHR-responsive gene called CYP1A6 in cells treated with AHR1 $\beta$  siRNA that were exposed to graded concentrations of TCDD, which induces CYP1A6 via the AHR.

### 2. TALENs: Gene-editing Nucleases

Considering the lack of specificity and transient, incomplete KD induced by siRNAs, we developed a protocol to generate AHR1 $\alpha$ <sup>-/-</sup>, AHR1 $\beta$ <sup>-/-</sup>, and double knockout XLK-WG cell lines using gene-editing proteins called transcription activator-like effector nucleases (TALENs). TALENs were engineered as plasmids controlled by the cytomegalovirus (CMV) promoter which, after transfection into XLK-WG cells, should induce double-strand breaks early in the second exon of AHR1 $\alpha$  and AHR1 $\beta$ .

## Basal AHR1 $\alpha$ and AHR1 $\beta$ mRNA Levels

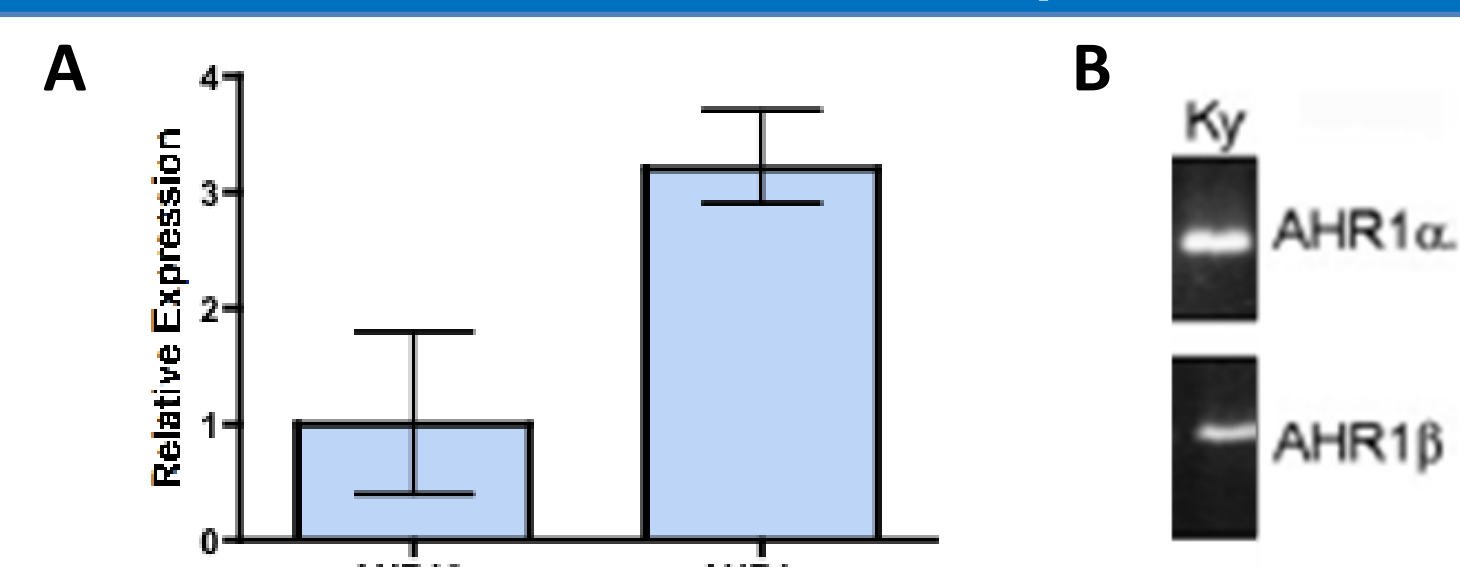


**Figure 2. AHR1 $\alpha$  mRNA is more abundant than AHR1 $\beta$  mRNA in *X. laevis* kidney tissue.** (A) RNA was isolated from near confluent XLK-WG cells and AHR1 $\alpha$  and AHR1 $\beta$  mRNAs were quantified by qRT-PCR in triplicates using the standard  $\Delta\Delta Ct$  method and  $\beta$ -actin as the endogenous control. Error bars represent the range of possible fold change values as defined by standard error of the  $\Delta Ct$ . (B) RNA was isolated from a whole *X. laevis* kidney and AHR1 $\alpha$  and AHR1 $\beta$  mRNAs were measured by semi-quantitative RT-PCR (Lavine et al., 2005).

## siRNA Knockdown of AHR1 $\alpha$ and AHR1 $\beta$

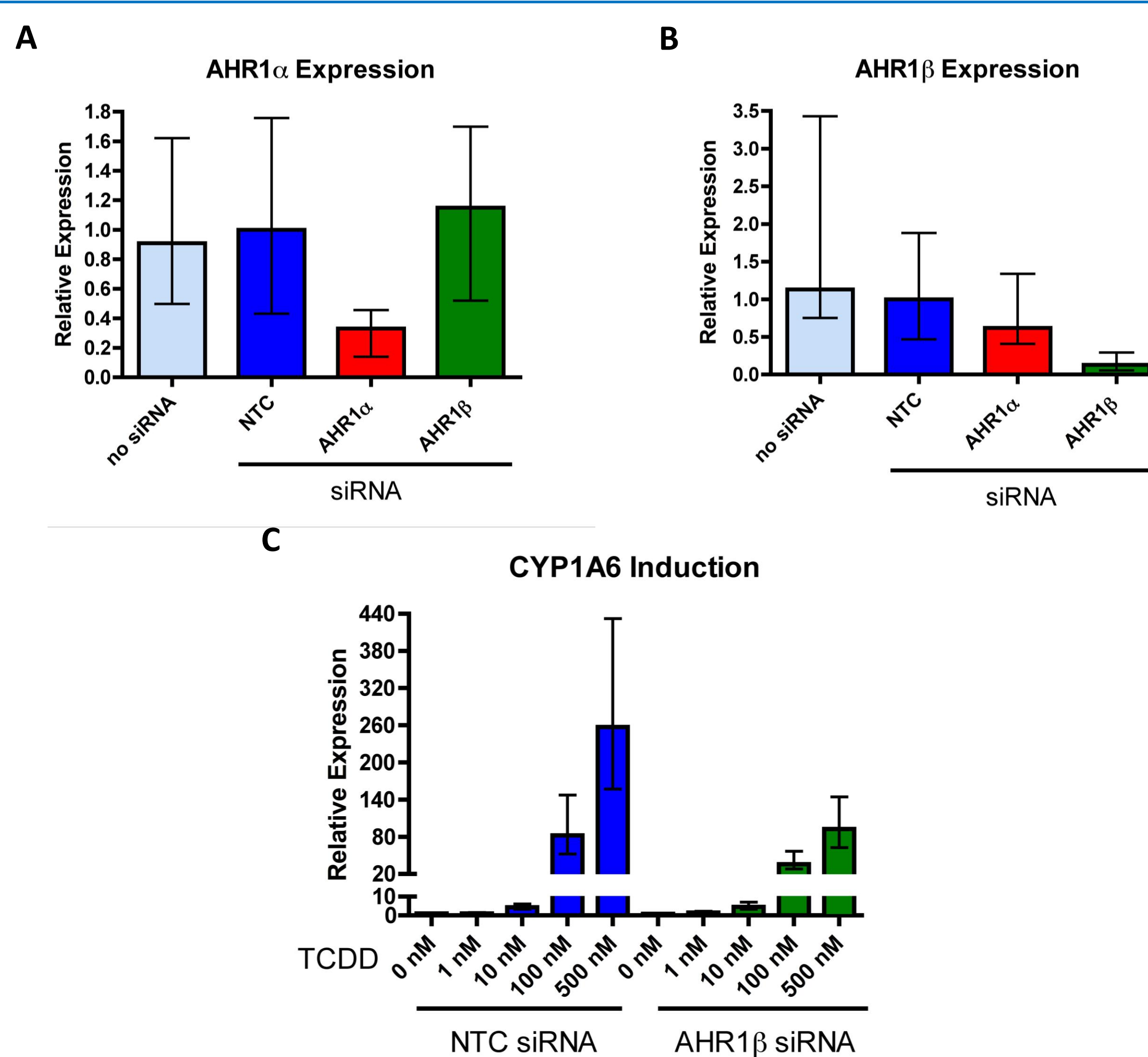


**Figure 3. AHR1 $\beta$  knockdown reduces TCDD-induced CYP1A6 mRNA expression.** (A-B) In 100  $\mu$ l cuvettes, 1 x 10<sup>6</sup> XLK-WG cells were transfected with 300 ng of either nontargeting control (NTC) siRNA, AHR1 $\alpha$ -targeted siRNA, AHR1 $\beta$ -targeted siRNA, or no siRNA, and seeded in 6-well plates. Total RNA was isolated 30 hr post-transfection. AHR1 $\alpha$  and AHR1 $\beta$  mRNAs were quantified by qRT-PCR in triplicates. (C) 3 x 10<sup>5</sup> cells were transfected with 300 ng of either NTC or AHR1 $\beta$  siRNA, seeded in 6-well plates, and exposed to graded concentrations of TCDD for 24 hr. 30 hr post-transfection, RNA was isolated and CYP1A6 mRNA was quantified by qRT-PCR in triplicates. AHR1 $\beta$  expression was reduced by 90% in siRNA treated cells (data not shown). For each experiment, relative expression values were determined by the standard  $\Delta\Delta Ct$  method using  $\beta$ -actin as the endogenous control. Error bars represent the range of possible fold change values as defined by standard error of the  $\Delta Ct$ .

### Conclusions:

The AHR1 $\beta$  siRNA is effective and paralog-specific. AHR1 $\beta$  knockdown reduces efficacy of CYP1A6 induction by TCDD. The AHR1 $\alpha$  siRNA is effective but not specific. It also causes decline in AHR1 $\beta$  transcript abundance.

## TALENs: Specific and Quantitative Knockout of AHR1 $\alpha$ and AHR1 $\beta$

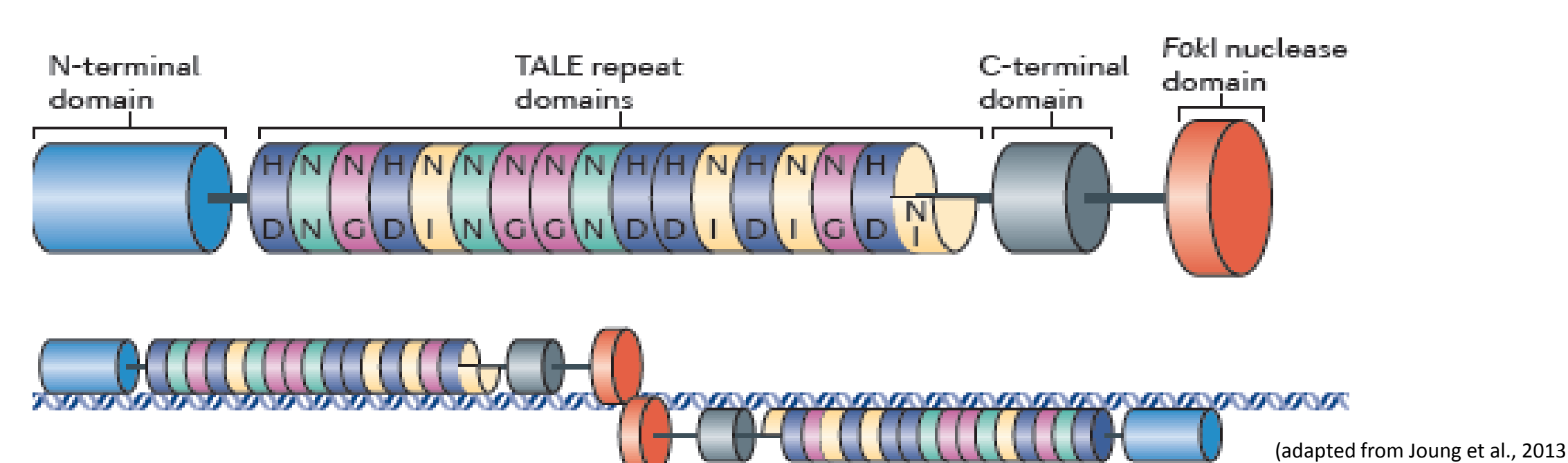


**Figure 4. TALEN construction and mechanism.** TALENs are composed of transcription activator-like effectors (TALEs), amino acid repeats engineered to bind a specific DNA sequence, and the FokI endonuclease. TALEN vectors must be transfected in pairs because FokI functions as a homodimer to generate a double-strand break. Imperfect repair of the break causes deletion of multiple nucleotides and disruption of the open reading frame to encode a short, non-functional protein.

We purchased three TALEN pairs from Collectis targeting: 1) AHR1 $\alpha$ , 2) AHR1 $\beta$  and, 3) both AHR1 $\alpha$  and AHR1 $\beta$ . Each TALEN pair targeted a region within the first 100 bp of exon 2 of either AHR1 $\alpha$  or AHR1 $\beta$ .

## Transfection Efficiency

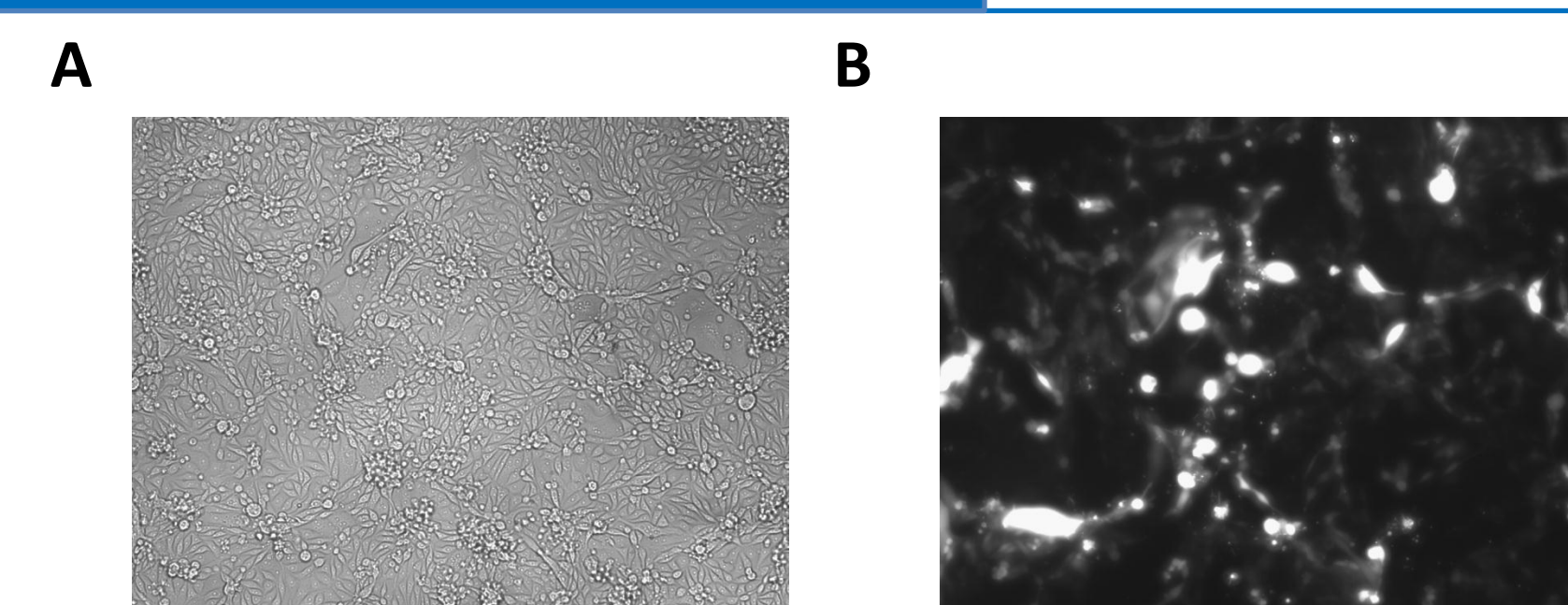


**Figure 5.** 1 x 10<sup>6</sup> XLK-WG cells were transfected with pmaxGFP vector (2  $\mu$ g, Lonza) using a nucleofector 4D. The next day, cell viability (A) and transfection efficiency (B) were assessed by brightfield and fluorescence microscopy using an Olympus IX-70 microscope. A representative field of view (100X magnification) is shown.

A ratio of fluorescent to viable cells was determined in three separate fields of view to quantify a transfection efficiency of ~30%. Cell counting was performed on images using a colony counter.

## Development and Analysis of AHR-Knockout Clonal Cell Lines

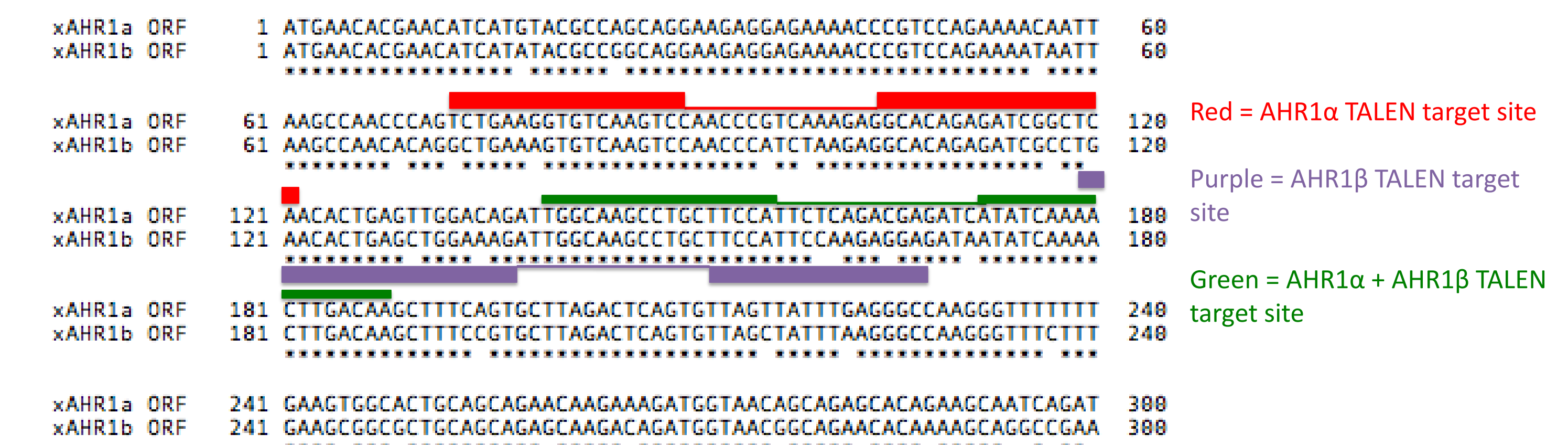
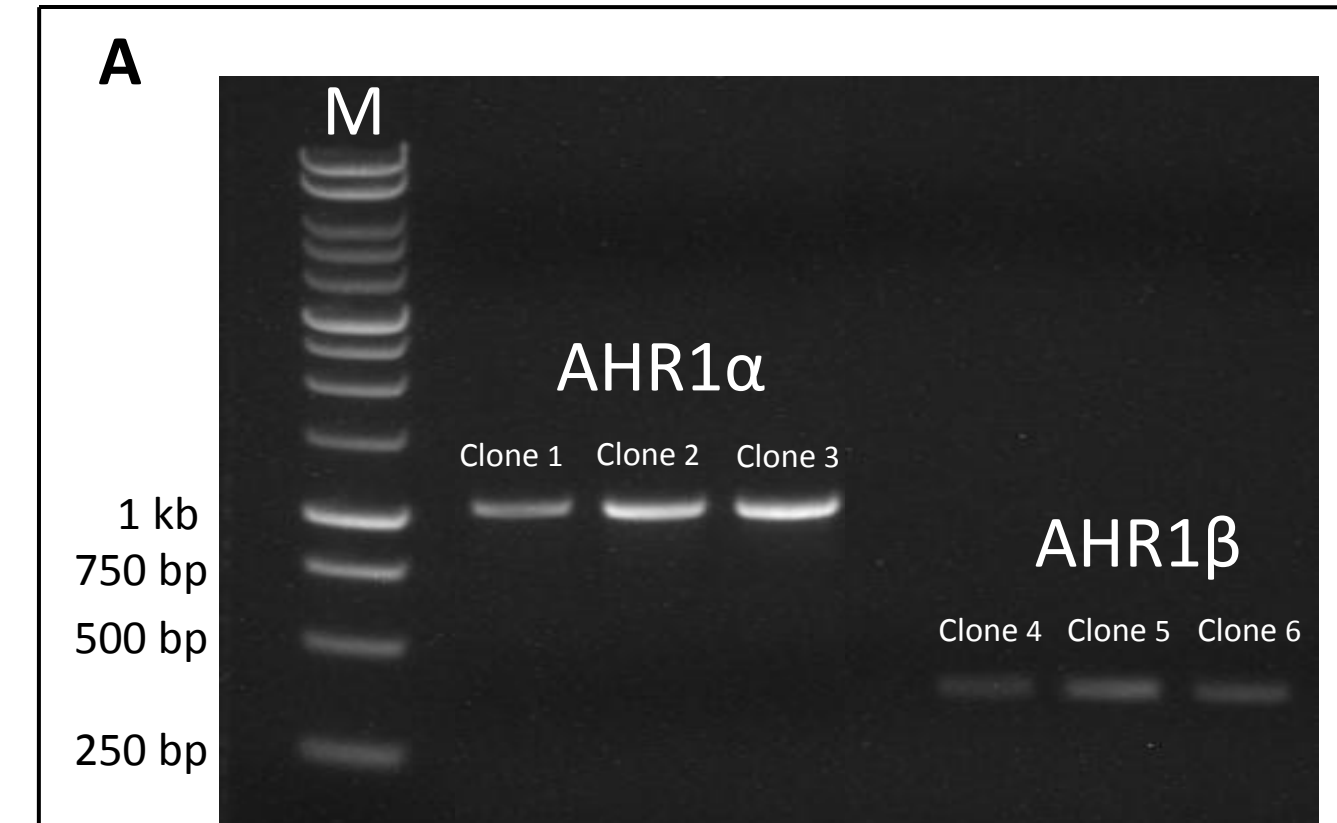


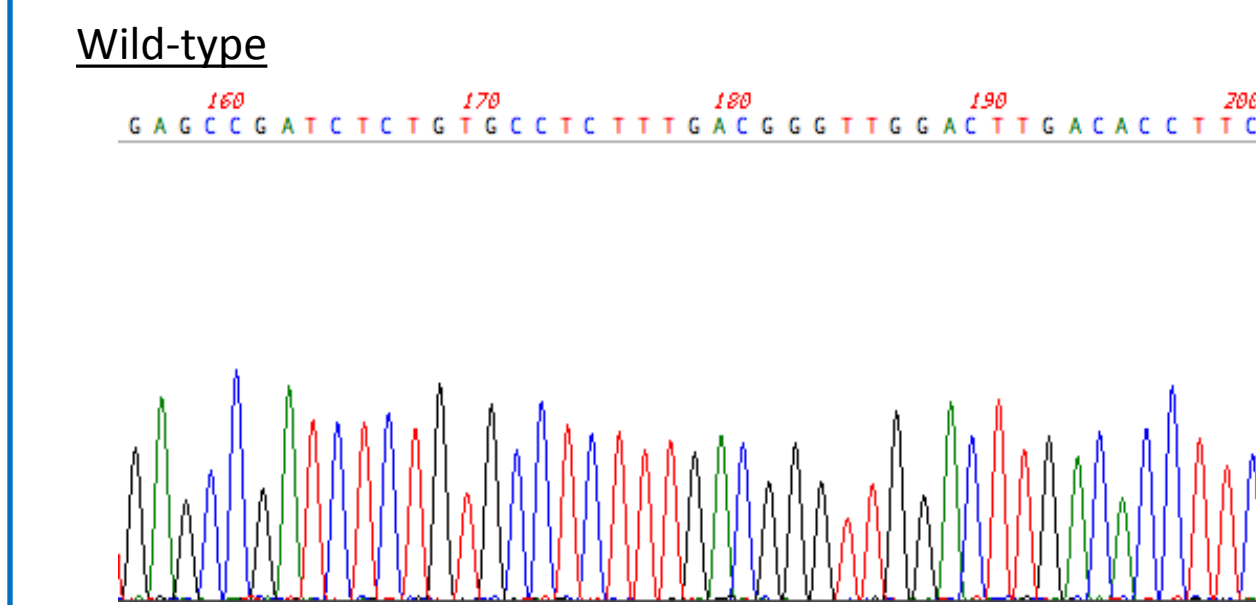
**Figure 6.** Nucleotide alignment of AHR1 $\alpha$  and AHR1 $\beta$  open reading frames annotated with TALEN target sites. FokI recognition sites (solid lines) are flanked by two TALE recognition domains (solid rectangles).

### Development of AHR-knockout clonal cell lines

**Step 1.** Cotransfect XLK-WG cells with TALEN and GFP plasmids  
**Step 2.** Seed cells in 96-well plates using a limiting dilution (0.6 cells/well).  
**Step 3.** Identify single GFP-positive cells and allow ~15 days for growth into colonies.  
**Step 4.** Transfer each cell colony to two new dishes - one for continued growth and a second for isolation of genomic DNA.  
**Step 5.** Amplify TALEN target sites at AHR1 $\alpha$  and AHR1 $\beta$  loci using PCR for sequencing.



### B



### D

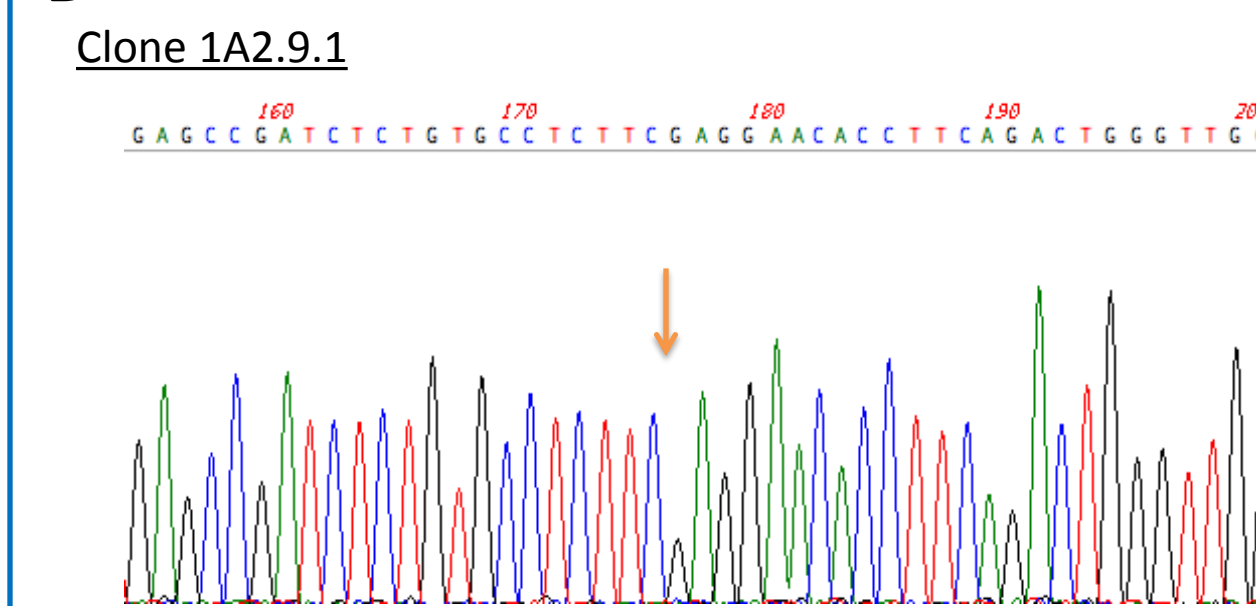
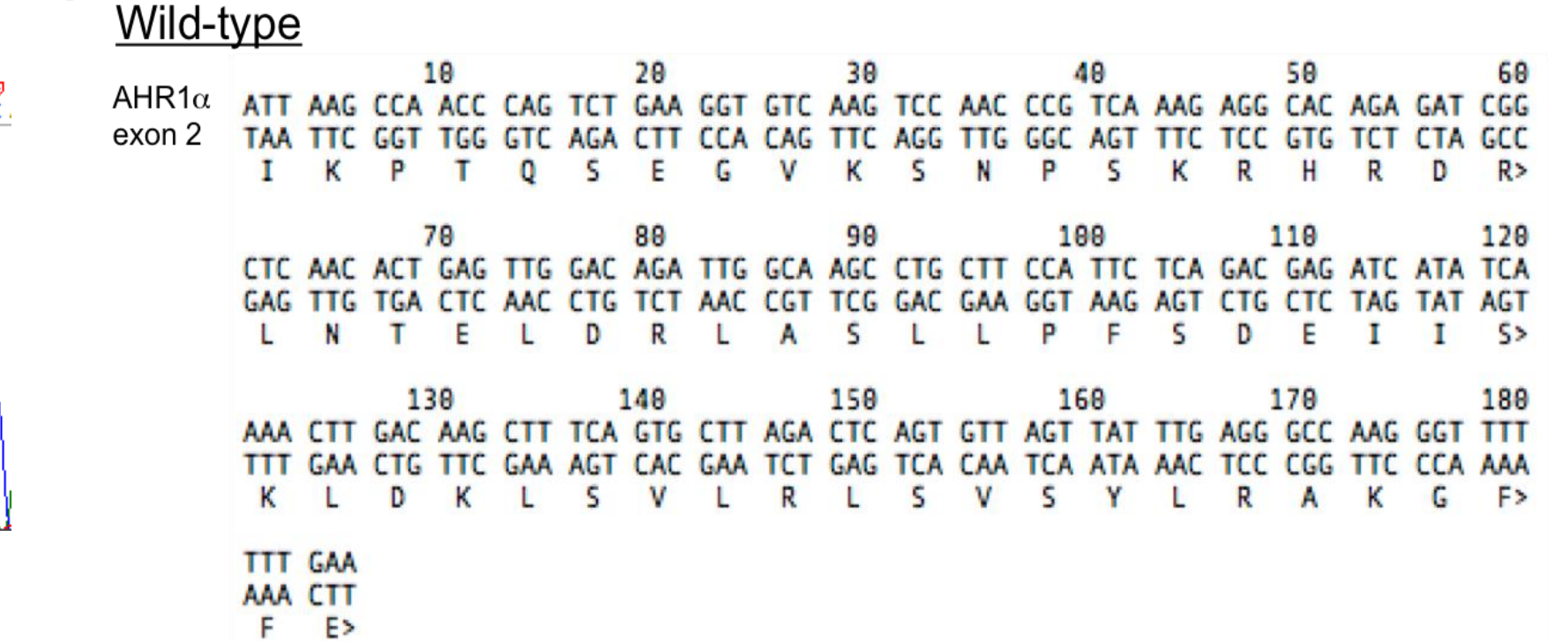
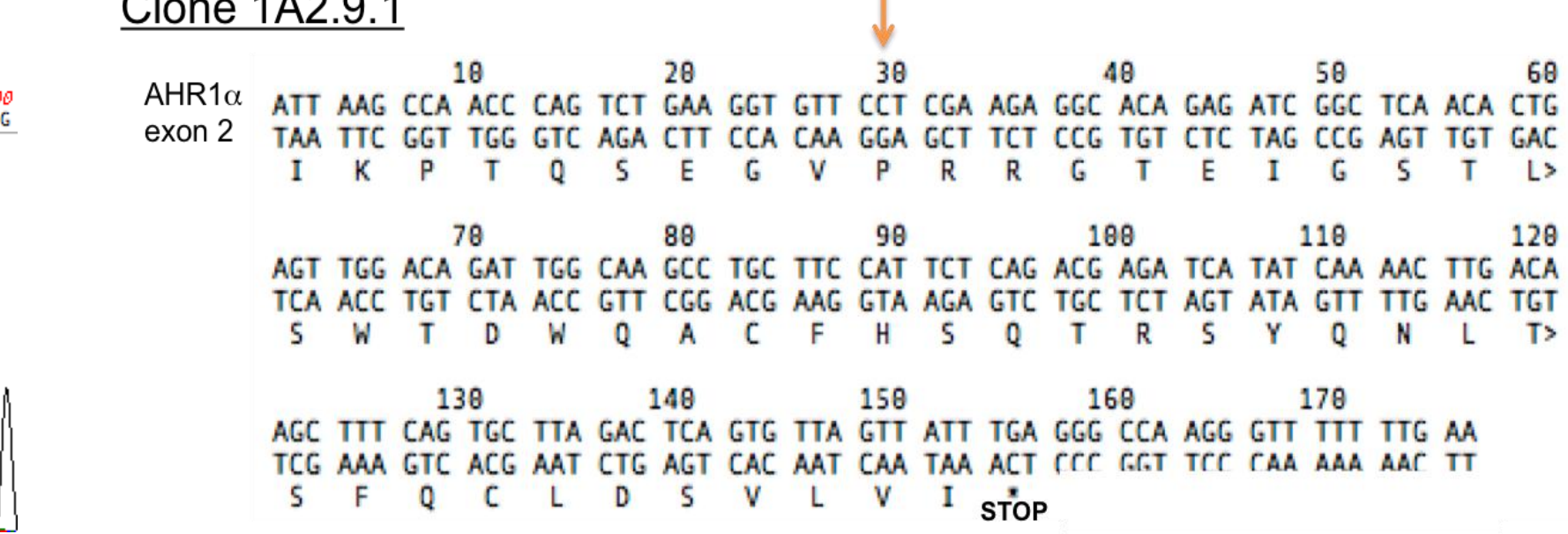


**Figure 7. Amplification and sequencing of TALEN target regions.** (A) Primers were designed to amplify a 1.1 kb region containing the AHR1 $\alpha$  TALEN target site and a 500 bp region containing the AHR1 $\beta$  TALEN target site. (B,D) Sequencing chromatograms of the AHR1 $\alpha$  TALEN target site in wild-type and 1A2.9.1 XLK-WG cells lines. Nucleotide annotations above each trace are the reverse complement of genomic DNA. (C,E) Sequences of genomic AHR1 $\alpha$  exon 2 in wild-type and 1A2.9.1 cells annotated with predicted amino acid sequences. Orange arrows correspond in sequence and indicate deviation from wild-type sequence. AHR1 $\alpha$  amino acid residue 71 is a STOP codon in 1A2.9.1 cells. (F) Number of potential mutant clones sequenced in this study.

### C



### E



clones sequenced	AHR1 $\alpha$ <sup>-/-</sup>	AHR1 $\beta$ <sup>-/-</sup>	double knockout
	68	20	12

## Summary and Future Work

### siRNA Experiments

XLK-WG cells lacking AHR1 $\beta$  exhibited a reduction in TCDD-induced CYP1A6 mRNA compared to control cells. This suggests that AHR1 $\beta$  is in part responsible for inducing this canonical AHR-responsive gene.

We will obtain a siRNA specific for AHR1 $\alpha$ , allowing us to reduce the gene's expression without affecting AHR1 $\beta$ . We can then investigate TCDD-induced CYP1A6 mRNA levels in cells lacking only AHR1 $\alpha$ .

### Developing AHR1 $\alpha$ <sup>-/-</sup>, AHR1 $\beta$ <sup>-/-</sup>, and Double Knockout XLK-WG Cell Lines Using TALENs

Using a GFP plasmid under the control of the same promoter as TALEN plasmids, we determined that transfection efficiency of plasmid DNA was ~30% in XLK-WG cells.

Of 68 potential AHR1 $\alpha$ -knockout cell lines sequenced, one clone, designated 1A2.9.1, harbored a 3 nt insertion coupled with a 13 nt deletion early in exon two of the AHR1 $\alpha$  open reading frame (Ant 83-100). The resulting frameshift causes an early STOP codon in the basic helix-loop-helix domain of AHR1 $\alpha$ .

Our preliminary siRNA data suggest that AHR1 $\alpha$  is capable of mediating CYP1A6 induction in response to TCDD (data not shown). Therefore, comparing CYP1A6 expression following TCDD exposure in 1A2.9.1 and WT cells will further verify the role of AHR1 $\alpha$  in the regulation of gene expression.

Unique expression of AHR1 $\alpha$  and AHR1 $\beta$  in various *X. laevis* tissues is evidence for spatial subfunctionalization of the paralogs. Recent studies of zebrafish AHRs used an AHR-knockout model and suggested similar subfunctional partitioning among paralogs (Garner et al., 2013; Goodale et al., 2012). Our future work will employ AHR-knockout *X. laevis* cell lines to define specific functions of AHR1 $\alpha$  and AHR1 $\beta$ .

## Acknowledgements

I thank Dr. Kathryn Edwards for her guidance in using the IX-70 microscope, Dr. Joan Slonczewski for allowing me to use her colony counter, and Scott Freiburg '16 for his support in the lab.

This work was supported by NIEHS grant ES011130 to WHP and the Kenyon College Summer Science program.

## References

- Garner, L., Brown, D., & Di Giulio, R. (2013). Knockdown of AHR1A but not AHR1B exacerbates PAH and PCB-126 toxicity in zebrafish Danio rerio embryos. *Aquat. Toxicol.* **142-143**, 336-346.
- Goodale, B., Lu, D., J., Bisson, W., Janssen, D., Waters, K., & Tanguay, R. (2012). AHR2 Mutant Reveals Functional Diversity of Aryl Hydrocarbon Receptors in Zebrafish. *PLoS ONE* **7**.
- Joung, J., & Sander, J. (2013). TALENs: a widely applicable technology for targeted genome editing. *Nature Reviews Molecular Cell Biology* **14**, 49-55.
- Lavine, J., Rowatt, A., Klimova, T., Whittington, A., Denler, E., Beck, C., & Powell, W. (2005). Aryl hydrocarbon receptors in the frog *Xenopus laevis*: two AHR1 paralogs exhibit low affinity for 2,3,7,8-tetrachlorodibenzo-*p*-dioxin (TCDD). *Toxicological Sciences* **88**, 60-72.